



Evaluation of polarimetric configurations for glacier classification

A. P. Doulgeris¹ , S. N. Anfinsen¹ , Y. Larsen² , K. Langley^{1,3} , T. Eltoft^{1,2}

¹ University of Tromsø, Norway,

² Norut AS, Tromsø, Norway

³ Norwegian Polar Institute, Tromsø, Norway





Outline



- Objectives
- Glacier facies
- Statistical models
- Classification algorithm
- Experimental findings
- Conclusion





Objectives



To investigate the classification information contained in different polarimetric channels

- Classification of an arctic glacier
- Quad, Dual and single polarisation combinations
- Supervised / unsupervised clustering
- Number of significant clusters



Polarimetry

- Full scattering matrix consists of combinations of sending and receiving, horizontal and vertical electromagnetic waves => complex scattering coefficients

$$\begin{bmatrix} E_h^r \\ E_v^r \end{bmatrix} = \frac{e^{jkr}}{r} \begin{bmatrix} S_{hh} & S_{hv} \\ S_{vh} & S_{vv} \end{bmatrix} \begin{bmatrix} E_h^t \\ E_v^t \end{bmatrix}$$

- Quad pol.: HH/HV/VH/VV channels
- Dual pol. modes: HH/HV, VH/VV, HH/VV
- Single pol. channels: HH, HV, VH and VV
- Reciprocity HV == VH

Glacier facies

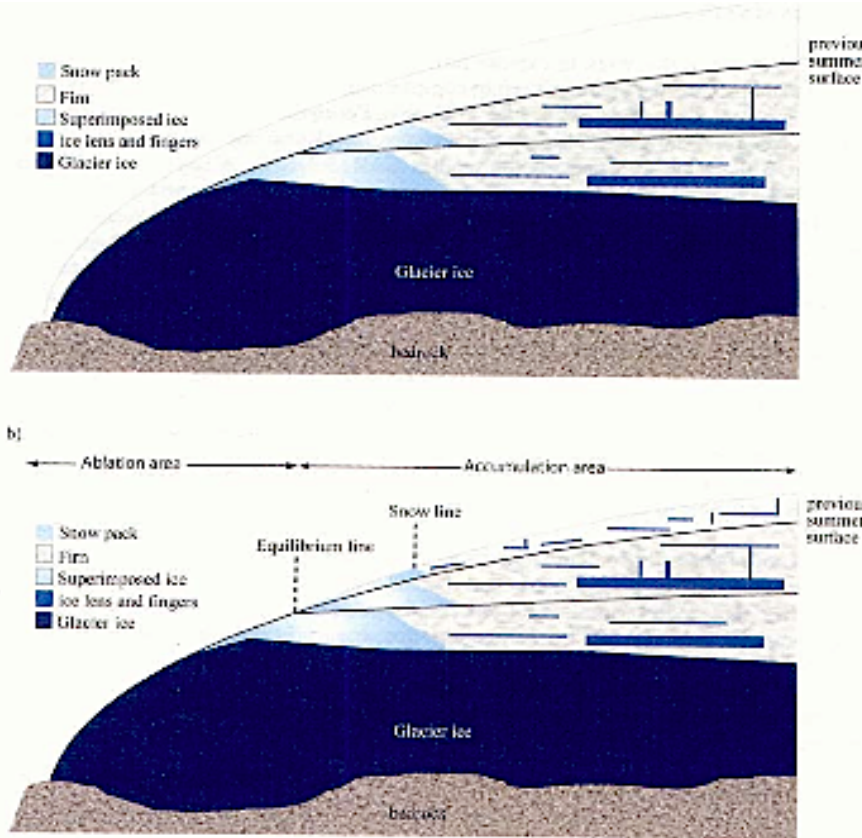


Fig. 1. Schematic cross section of a glacier indicating the different glacial facies and zones. a) spring, b) end of summer.

- Firn accumulation zone
 - Never fully melts
 - Seasonal layers of compacted snow/ice
- Superimposed ice zone
 - Seasonal melt/re-freeze cycles
 - Very rough
- Glacial ice zone
 - Melting removes ice

GPR traces of glacier facies

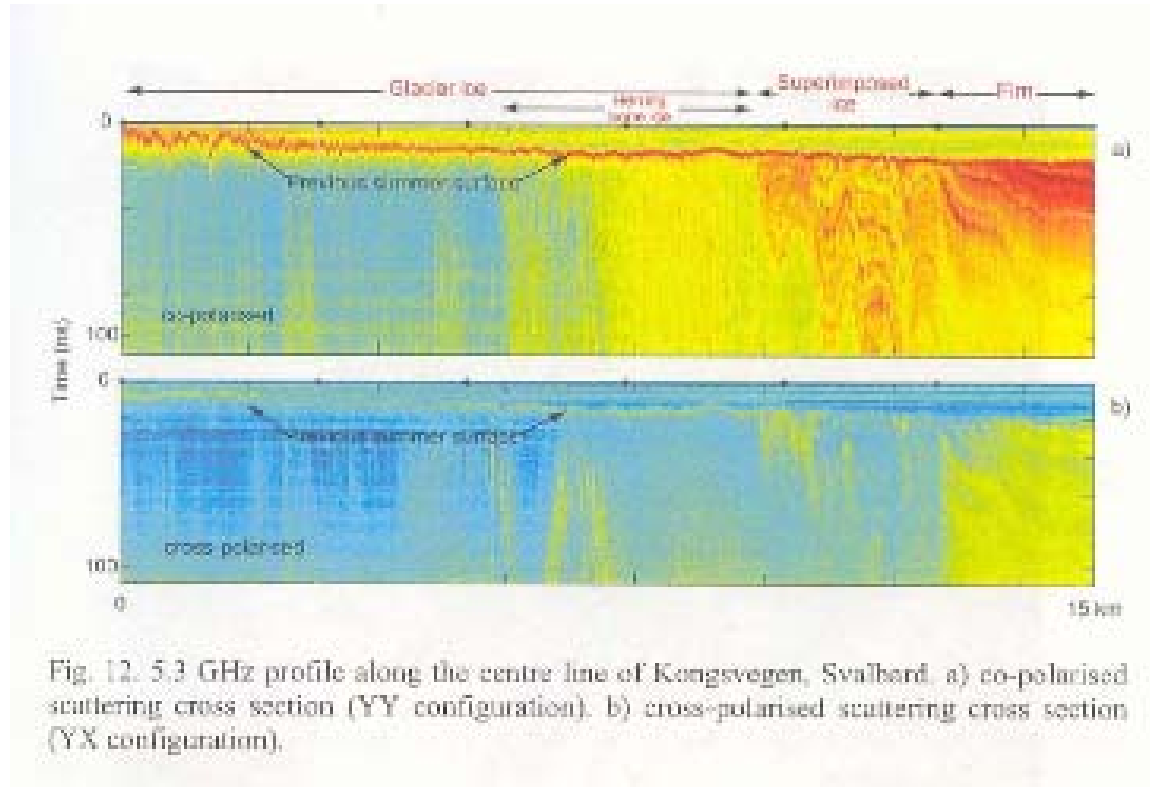


Fig. 12. 5.3 GHz profile along the centre line of Kongsvegen, Svalbard. a) co-polarised scattering cross section (YY configuration). b) cross-polarised scattering cross section (YX configuration).

Statistical models

- Gaussian scattering coefficients
 - Wishart covariance matrix
 - Speckle only, no texture
- Non-Gaussian, multivariate K-distribution for scattering coefficients
 - Product model, Gamma distributed texture
$$\mathbf{y} = \sqrt{z}\mathbf{\Gamma}^{\frac{1}{2}}\mathbf{x}$$
 - K-Wishart covariance matrix
 - Incorporates textural variation

Statistical models

Standard Wishart:

$$f_{\mathbf{C}}(\mathbf{C}; L, \boldsymbol{\Sigma}) = \frac{L^{Ld} |\mathbf{C}|^{L-d} \exp(-L \operatorname{tr}(\boldsymbol{\Sigma}^{-1} \mathbf{C}))}{|\boldsymbol{\Sigma}|^L I(L, d)}$$

where

$$I(L, d) = \pi^{\frac{d(d-1)}{2}} \prod_{i=1}^d \Gamma(L - i + 1)$$

K-Wishart distribution:

$$f_{\mathbf{C}}(\mathbf{C}; L, \alpha_L, \mu_L, \boldsymbol{\Gamma}) = \frac{2 |\mathbf{C}|^{L-d}}{I(L, d) \Gamma(\alpha_L)} \left(\frac{L \alpha_L}{\mu_L} \right)^{\frac{\alpha_L + Ld}{2}} (\operatorname{tr}(\boldsymbol{\Gamma}^{-1} \mathbf{C}))^{\frac{\alpha_L - Ld}{2}} \times K_{\alpha_L - Ld} \left(2 \sqrt{\frac{L \alpha_L}{\mu_L} \operatorname{tr}(\boldsymbol{\Gamma}^{-1} \mathbf{C})} \right).$$

Scalar observable

Mean squared Mahalanobis distance

$$M = \text{tr}(\hat{\Sigma}^{-1} \mathbf{C}) = \frac{1}{L} \sum_{l=1}^L (\mathbf{y}_l^H \Sigma^{-1} \mathbf{y}_l)$$

$$\mathcal{E}\{M\} = d$$

$$\text{var}(M) = \frac{1}{L} \left(d + \frac{d(d+1)}{\alpha} \right)$$



Classification algorithm

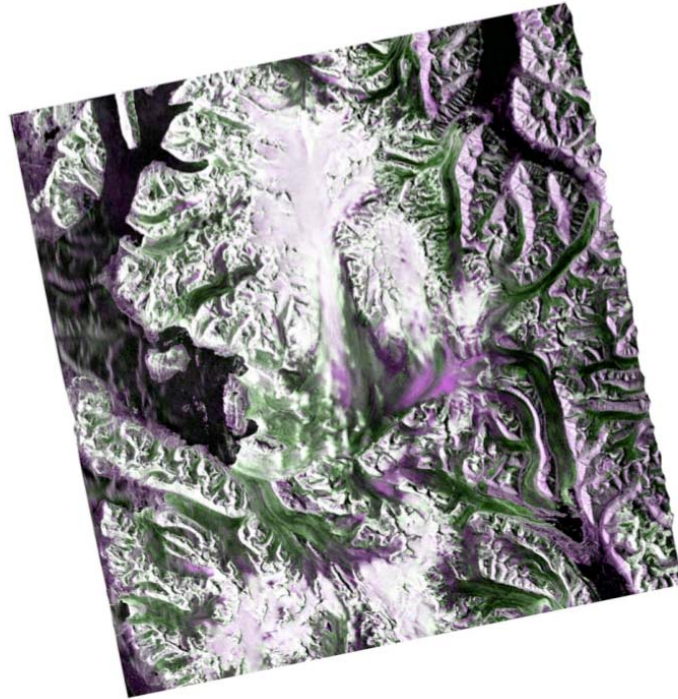


1. Determine appropriate number of classes
2. Make an initial partitioning using K-means on diagonal intensities
3. Estimate initial class parameters
4. Estimate class posterior probabilities (membership weights) under model
5. Re-estimate model parameters based on weighted sums
6. Return to 4, and continue until convergence

A.P. Doulgeris, S.N. Anfinsen, and T. Eltoft. Classification with a non-gaussian model for polsar data. *Geoscience and Remote Sensing, IEEE Transactions on*, 46(10):2999–3009, Oct. 2008.



Geographic location



ALOS L-band SAR image covering Ny-Ålesund area.

(Data provided by European Space Agency)



Holtedahlsfonna glacier



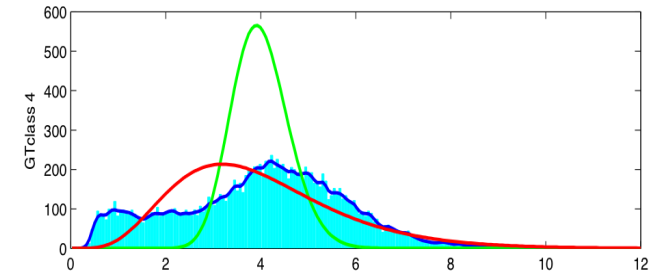
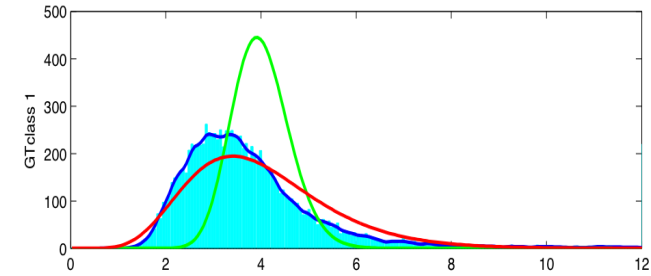
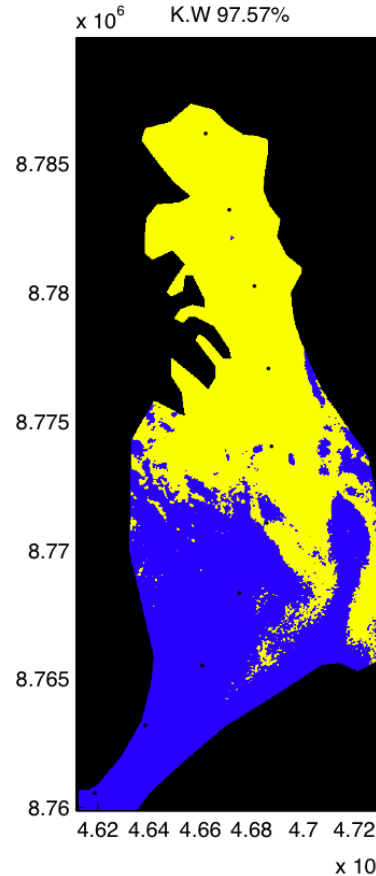
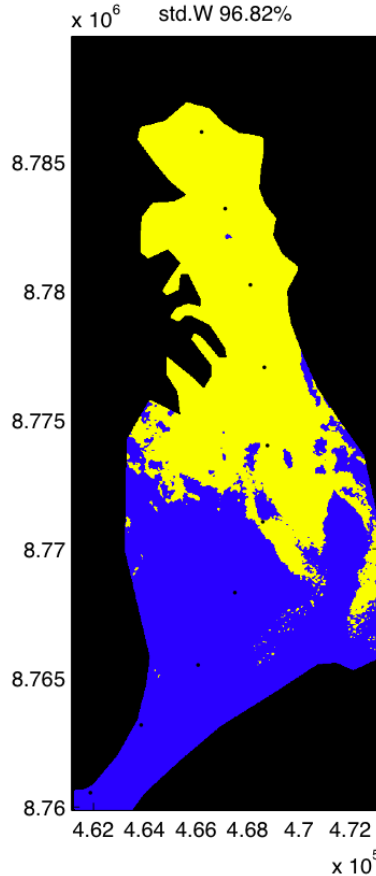
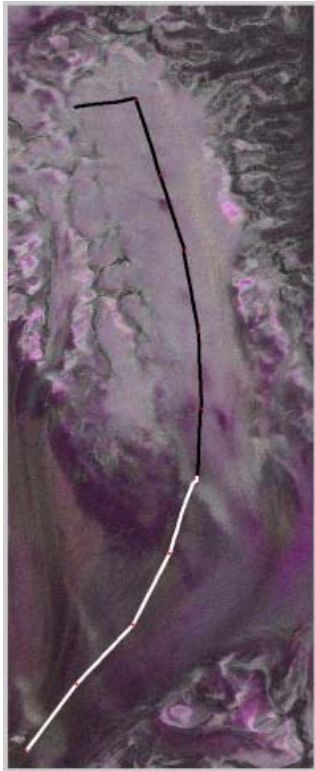
Experimental findings



- Supervised classification
 - Approx. 97% accuracy for both models
 - Not a good fit to either model
 - Inadequate ground truth data
- Unsupervised clustering
 - Number of classes by visual trial and error
 - K-Wishart a good fit to class histograms
 - Wishart not usually a good fit, needs more classes
- Evaluated for all combinations of polarimetric channels

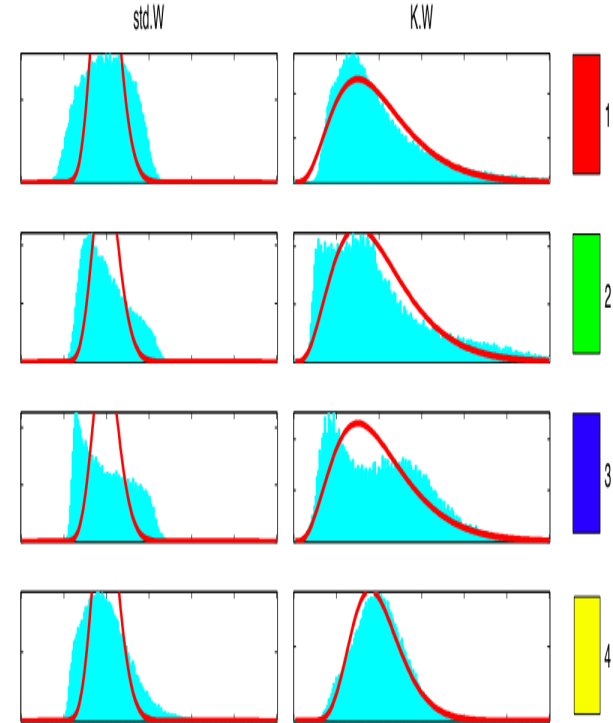
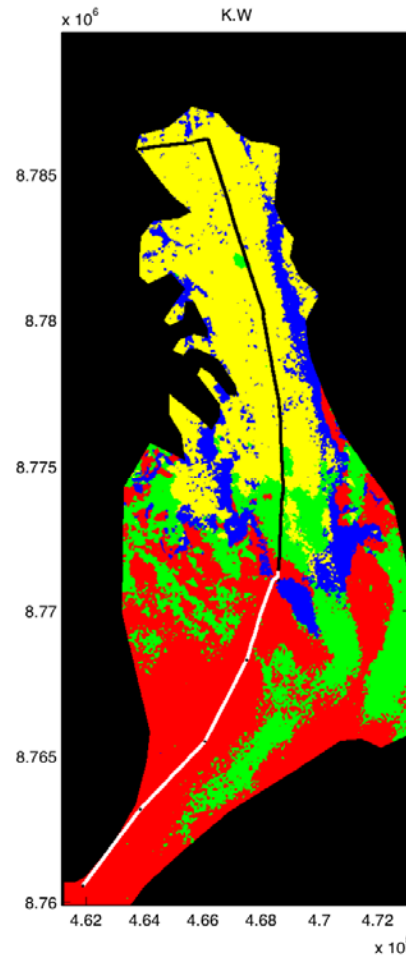
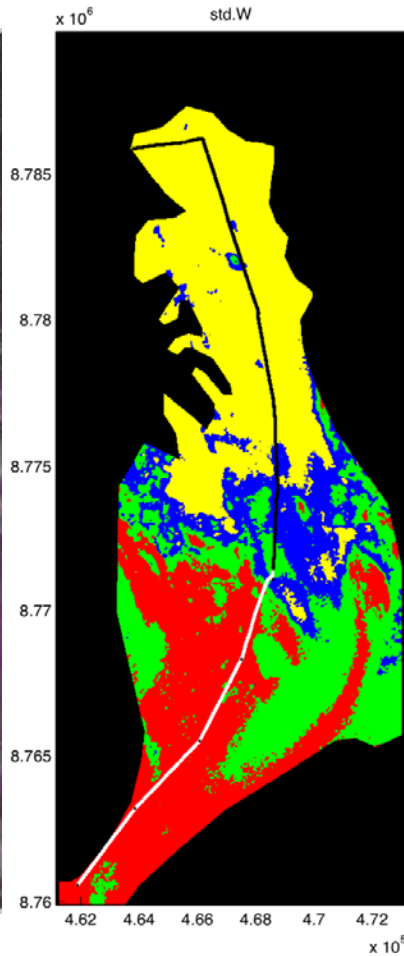
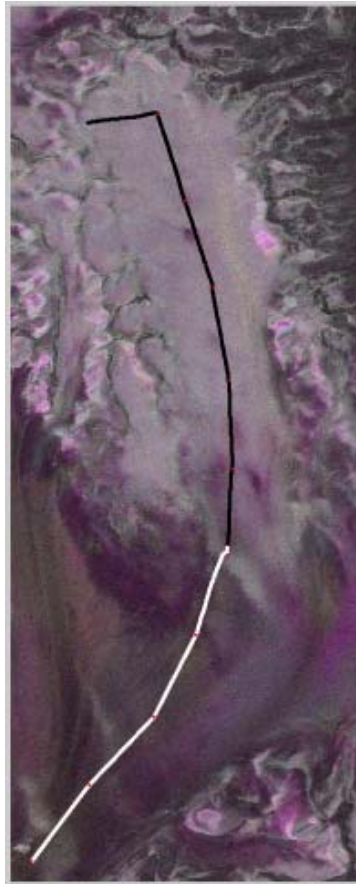


Supervised Classification

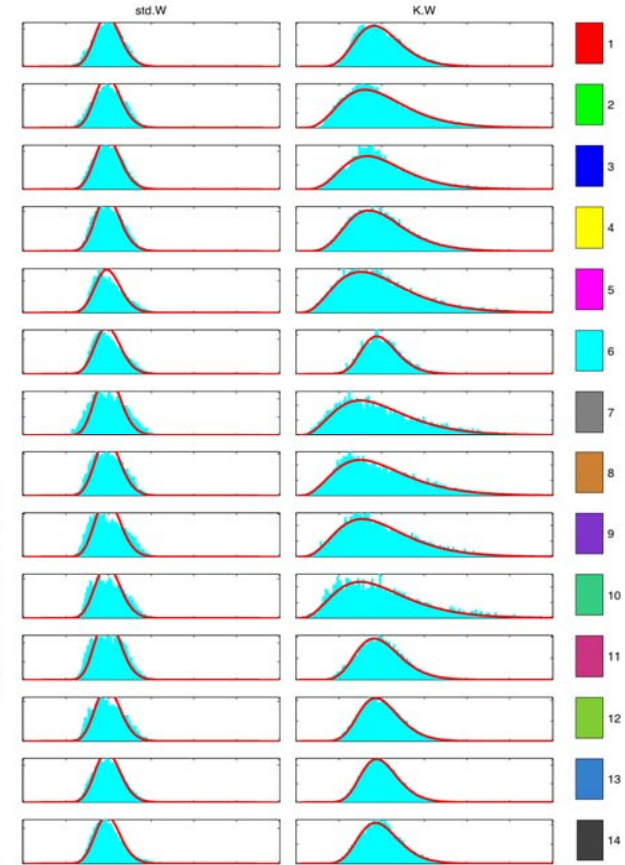
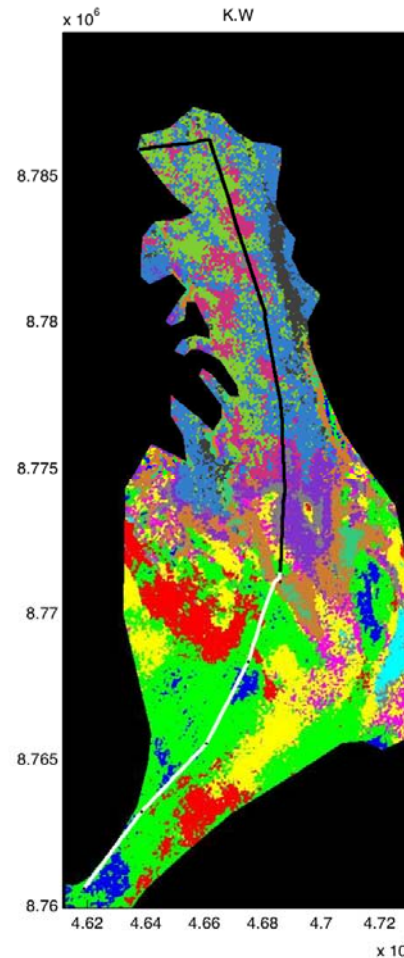
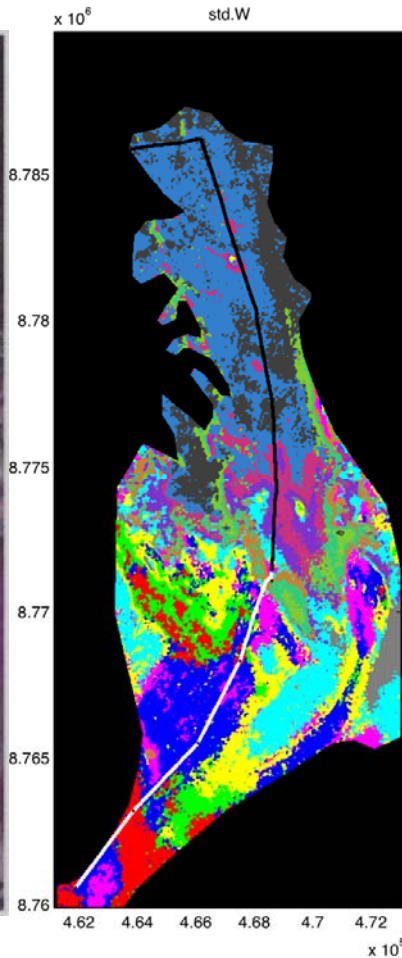
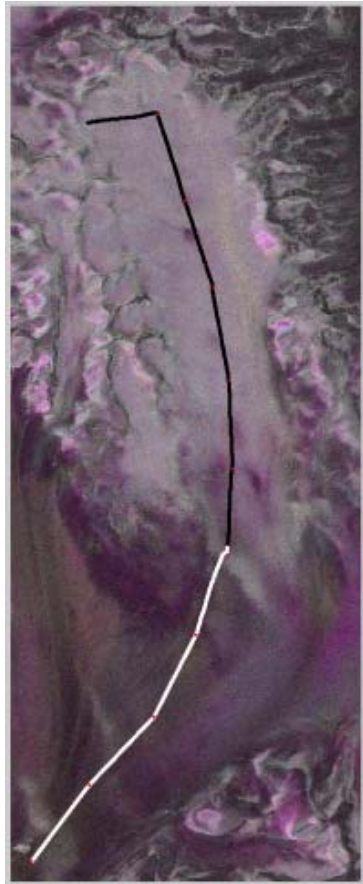


Class histograms (filled blue) with both model curves, Wishart in green and K-Wishart in red.

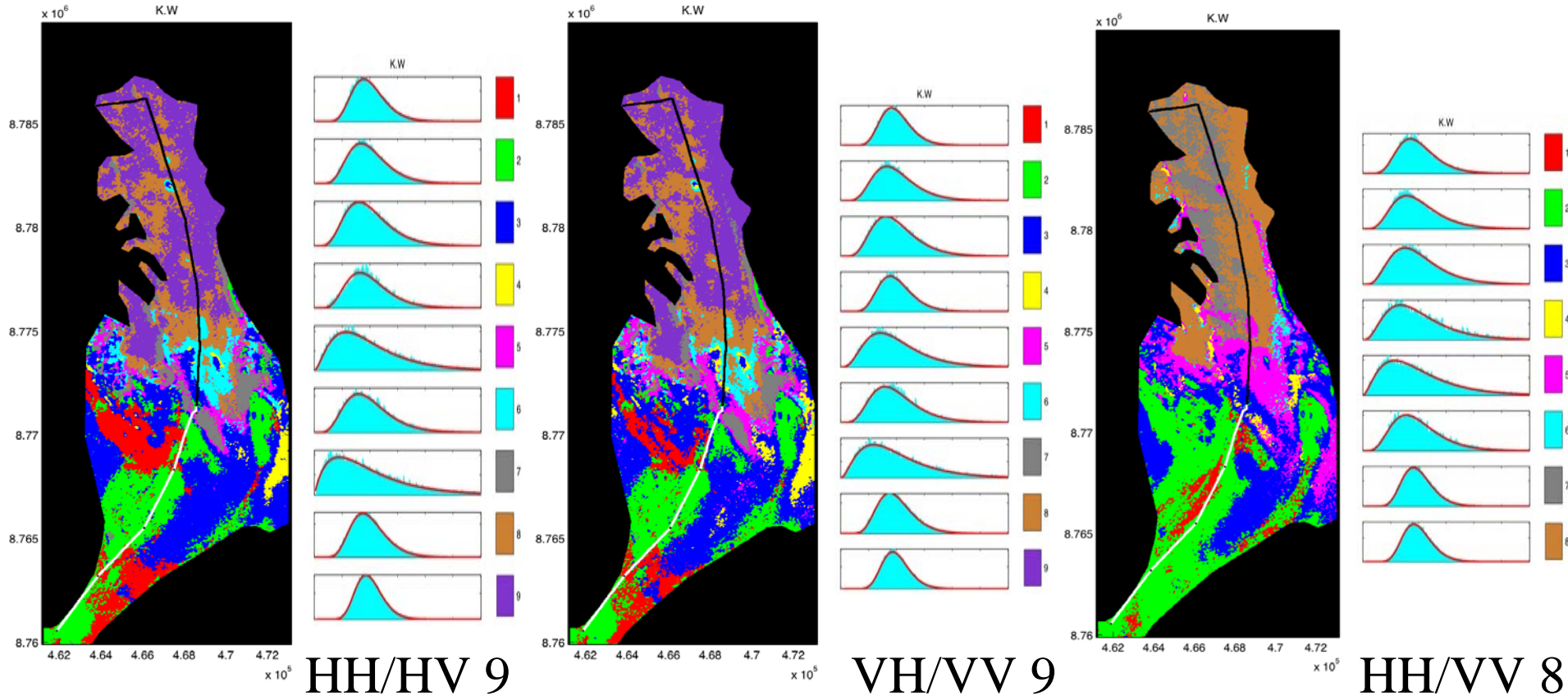
Unsupervised: Quad 4



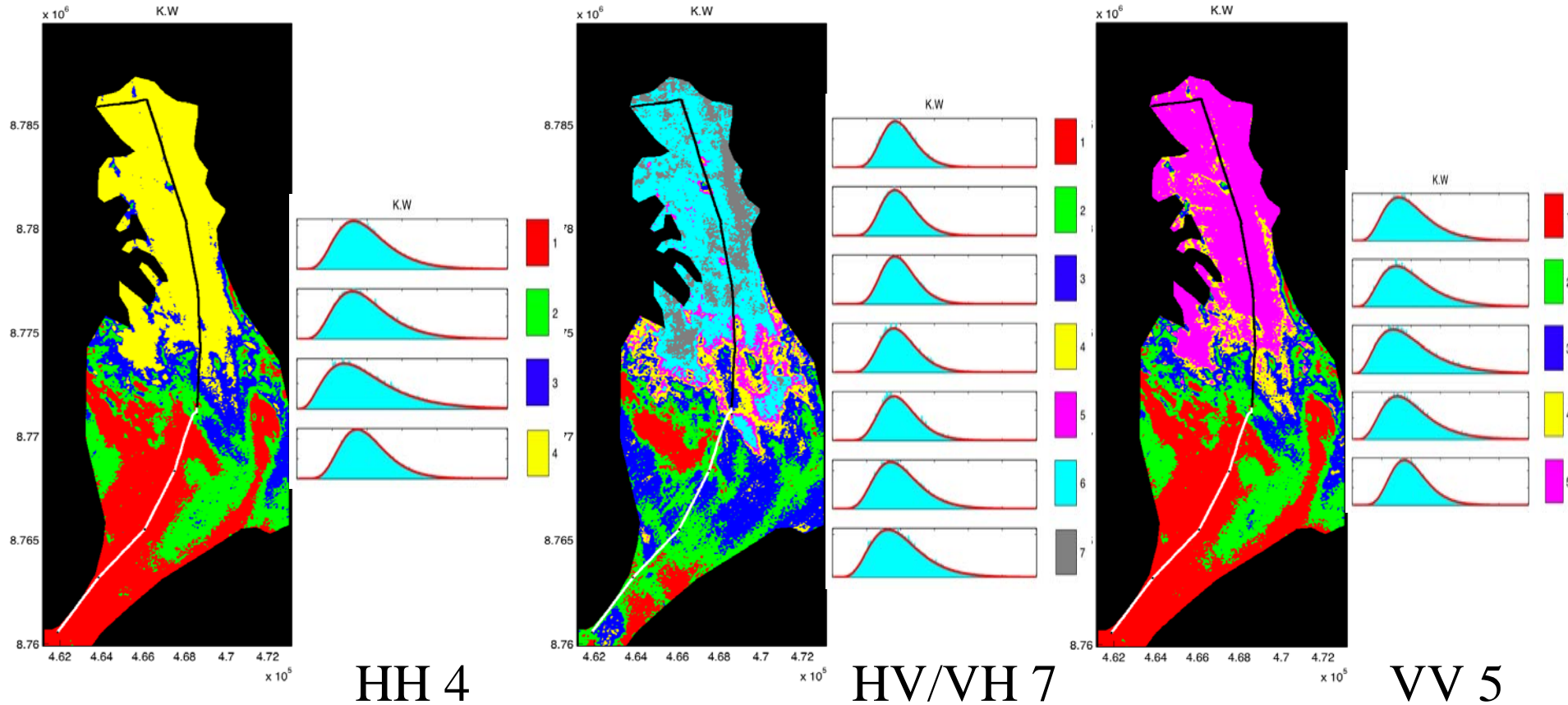
Unsupervised: Quad 14



Unsupervised K-W: Dual pols.



Unsupervised K-W: Single pol.





Number of classes



Combination	# of classes
Quad.	14
Dual HH/HV	9
Dual VH/VV	9
Dual HH/VV	8
Single HH	4
Single HV/VH	7
Single VV	5





Conclusion

- We have clearly demonstrated the quite detailed natural clusters visible in PolSAR images of glacier ice.
- The histogram fitting indicates significant non-Gaussian clusters which the K-Wishart model appears to fit very well.
- We have measured the reduced information content, via fewer distinct clusters, when using incomplete polarimetric data sets.





Future research



- Glaciologists perspective on the many sub-classes.
- Interpretation of the clusters via polarimetric decompositions.
- Validation of the clustering results via detailed ground based field work.
- Rigorous statistical goodness-of-fit tests to automate choice of number of classes.

